


Performance of rubber mortars containing silica coated rubber

 J. Li ^a,  P. Chen^{a, b} ,  H. Cai^a,  Y. Xu^a,  X. Tian^a,  C. Li^b,  L. Cui^a

a. School of Civil Engineering and Architecture, Anhui University of Science and Technology, (Huainan, China)
b. Jitoo UHPC (Shandong) New Material Technology Co., Ltd, Shandong Academician Workstation of Ghani Razaqpur, (Weihai, China)
 peiyuan29@126.com

Received 22 September 2020
Accepted 16 November 2020
Available on line 20 May 2021

ABSTRACT: This paper investigates the influence of silica coated rubber on the performance of rubber mortars. A classical Stöber sol-gel method is applied to produce a layer of silica coating on rubber particles, which is used to partially replace the fine aggregates in concrete. The effects of the surface-modified rubber particles on the flowability, mechanical strength, capillary water absorption rate, and microstructure of mortars are examined. The results show that the silica coating on the rubber particles reduces the contact angle between the rubber particles from 120° to 103° (i.e., by 17°) and changes the hydrophobic properties from strong hydrophobicity to weak hydrophobicity. The mechanical strengths of mortars are significantly improved by the incorporation of surface-modified rubber particles, i.e., from 41.60% to 44.86% (compressive strength) and from 7.80% to 26.28% (flexural strength). In addition, the incorporation of surface modified rubber particles increases the density of the mortar's microstructure and enhances the interfaces with its surrounding pastes.

KEY WORDS: Mortar; Waste treatment; Mechanical properties; Characterization; Microstructure.

Citation/Citar como: Li, J.; Chen, P.; Cai, H.; Xu, Y.; Tian, X.; Li, C.; Cui, L. (2021) Performance of rubber mortars containing silica coated rubber. *Mater. Construcc.* 71 [342], e244. <https://doi.org/10.3989/mc.2021.11620>.

RESUMEN: *Rendimiento de morteros de caucho que contienen caucho recubierto de sílice.* Este trabajo investiga la influencia del caucho recubierto de sílice en el rendimiento de los morteros de caucho. Se aplica un método clásico de Stöber sol-gel para producir una capa de revestimiento de sílice sobre las partículas de caucho, que se utiliza para reemplazar parcialmente los áridos finos en el hormigón. Se examinan los efectos de las partículas de caucho modificadas en la superficie sobre la fluidez, la resistencia mecánica, la tasa de absorción de agua por capilaridad y la microestructura de los morteros. Los resultados muestran que el revestimiento de sílice de las partículas de caucho reduce el ángulo de contacto entre las partículas de caucho de 120° a 103° (es decir, en 17°) y cambia las propiedades hidrofóbicas de hidrofobia fuerte a hidrofobia débil. Las resistencias mecánicas de los morteros mejoran significativamente con la incorporación de partículas de caucho modificadas en la superficie, del 41,60% al 44,86% (resistencia a la compresión) y del 7,80% al 26,28% (resistencia a la flexión). Además, la incorporación de partículas de caucho modificadas en la superficie aumenta la densidad de la microestructura del mortero y mejora las interfases con las pastas que lo rodean.

PALABRAS CLAVE: Mortero; Tratamiento de residuos; Propiedades mecánicas; Caracterización; Microestructura.

Copyright: ©2021 CSIC. This is an open-access article distributed under the terms of the Creative Commons Attribution 4.0 International (CC BY 4.0) License.

1. INTRODUCTION

Currently, waste tires have become one of the main sources of waste flow worldwide, causing great concern about the related environmental problems. Effective methods to reuse waste tires are of interest to many people. One of the recommended reuse routes for waste tires is to convert them into rubber particles as a possible alternative to the fine aggregates in concrete (1, 2). Related studies have indicated that concrete containing rubber particles exhibits a better impact resistance, toughness, thermal insulation, and sound absorption, which are specially required in the construction of airports, surge guards and military protection (3-5). This study provides reliable insights into the recycling of waste tires into useful new materials. However, concrete containing rubber particles normally has a poor mechanical performance (6). It was reported that adding rubber to concrete caused the concrete to lose 20% to 60% of its compressive strength depending on factors such as the mix proportion, the nature of the rubber particles, and the ages of the rubber particles and the concrete (7). The low elasticity modulus and hydrophobic nature of rubber particles are the two major reasons for the reduction in the compressive strength of rubber concrete (8). Since rubber particles undergo larger deformations than pastes under the same load, the stress transferring route of rubber concrete's bearing load breaks at the interface. From this point of view, the rubber particles within the microstructure of the concrete may substantially function as pores (9, 10).

To overcome this disadvantage of rubber concrete, modifying the rubber particles is one potential method of enhancing the bonding effect of the rubber particles at the interface. Actually, the surface modification of rubber particles has been found to be an effective method of improving the mechanical strength of rubber concrete (11). Li *et al.* (12) modified rubber particles using a silane coupling agent, and they found that the compressive strength and flexural strength of the rubber concrete increased by 4% and 13%, respectively. Dong *et al.* (13) confirmed that mortars containing rubber treated with a silane coupling agent had 10-20% higher compressive strengths. Balaha *et al.* (14) showed that treating crumb rubber with polyvinyl alcohol (PVA), silica fumes and sodium hydroxide (NaOH) reduced the reductions in the compressive strength and tensile strength of the concrete compared to concretes containing untreated crumb rubber. He *et al.* (15) introduced carboxyl, hydroxyl and sulfonic acid groups onto the rubber surfaces using KMnO_4 and NaHSO_3 solutions. They found that the contact angle of the modified rubber was reduced, which improved the compressive strength a maximum of 48.7%.

In addition to chemical surface modification of rubber particles, chemical coating is another feasible route (11). This method forms a layer of coating

on the surface of the substance through a chemical reaction to improve the performance of the material's surfaces and to enhance its compatibility with other substrates. The sol-gel method is widely used for chemical coating due to its mild reaction and low cost (16). It has been investigated and applied to the coating of microcapsules and other various multidimensional fields, such as the ceramic industry and biomedical instruments (17-22). Nevertheless, its use has rarely been reported in the context of concrete materials.

Thus, in this study, the sol-gel method was used to coat rubber particles with silica. This method not only enhances the bonding effect between the rubber particles and the surrounding pastes, but it also greatly inhibits the aggregation of rubber particles within mixtures. To investigate the benefits of modifying mortars with rubber, sand volume fractions of 5%, 10%, 15%, and 20% were replaced by rubber particles. A comprehensive experiment was conducted to investigate the effects of the surface-modified rubber particles on the performance of the mortars. The fresh and hardened properties of the mortars were tested including the flowability, compressive strength, and capillary water absorption. In addition, scanning electron microscopy (SEM) photographs, X-ray diffraction (XRD) and Fourier transform infrared spectroscopy (FT-IR) were used to reveal the related mechanisms.

2. EXPERIMENTAL DETAILS

2.1. Materials

The P.O. 42.5 ordinary Portland cement produced according to standard ASTM C150/C150M (23) was purchased from the Anhui Conch Cement Co., Ltd. Table 1 shows its density, Brunauer, Emmett and Teller (BET) area and chemical composition. The aggregate used was natural river sand with a fineness modulus of 2.36 and an apparent density of 2600 kg/m^3 . Rubber particles (60 - 80 mesh) produced from waste tires were substituted for part of the sand volume (Figure 1). The particle size distributions of the cement, rubber particles and sand are presented in Figure 2. Unless otherwise noted, the water used to prepare the pastes and mortars was tap water.

The experiments involved a method of surface coating the rubber particles. The materials used in these experiments were deionized water, analytically pure orthosilicic acid tetraethyl ester (TEOS), ammonia hydroxide with an ammonia concentration of 25%, anhydrous ethanol, and 3-aminopropyltriethoxysilane (silane coupling agent KH550) with effective contents of greater than 98%. All of those materials were purchased from the Sinopharm Chemical Reagent Co., Ltd.

TABLE 1. Density, BET area and chemical composition of the cement.

	Density / (kg/m ³)	BET area / (m ² /g)	Chemical composition/(wt.%) (XRF)					
			CaO	SiO ₂	Al ₂ O ₃	MgO	Fe ₂ O ₃	SO ₃
Cement	3100	1.081	60.22	21.07	8.82	1.36	3.65	2.81

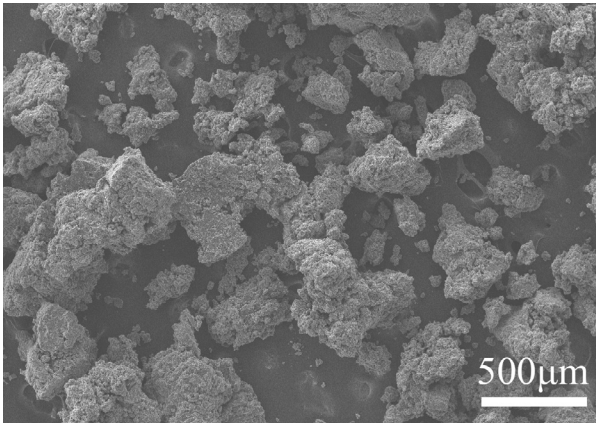


FIGURE 1. SEM images of the rubber particles.

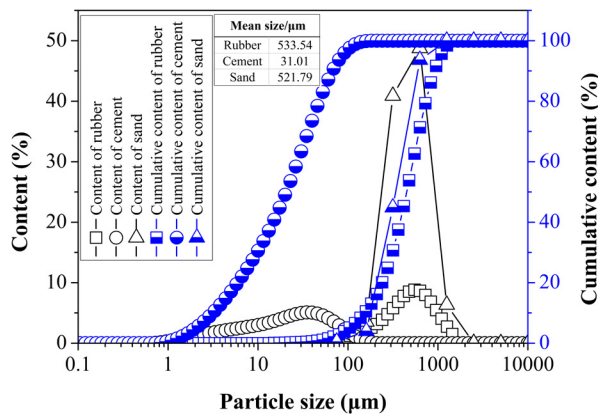


FIGURE 2. Particle size distributions of the cement, rubber particles and sand.

2.2. Surface modification of the rubber particles

The classical Stöber sol-gel method was used to modify the surface properties of the rubber particles. In a typical procedure, 60 mL of ethanol, 5 mL of deionized water, 5 mL of ammonia water, 15 mL of TEOS, 20 g of rubber particles and 0.171 g of KH550 were mixed together. They were stirred for 4 h at room temperature and pressure and were subsequently aged for 24 h. Then, the mixture was filtered, washed with alcohol and water, and the rubber particles were separated out using a Buchner funnel. Finally, the surface modified rubber particles were oven dried at 60 °C for 24 h.

2.3. Mixture proportions

To examine the effect of the surface modified rubber particles on the performance of the mortar, 9 mixtures were prepared with sand content of 50%. A water to cement (w/c) ratio of 0.4 was selected to ensure suitable workability of mortar samples. Rubber particles with and without surface modification were used to substitute for 5% to 20% of the sand volume (Table 2). For the codes of these mixtures, R indicates mortar containing raw rubber and SMR indicates mortar containing surface modified rubber, and the numbers following the letter identifications indicate the volume of sand replaced by rubber particles with or without surface modification. To prepare the mortars, all of the dry materials were initially mixed in a Harbor mixer for 3 min, and then, they were mixed with water and were stirred for 2 min.

TABLE 2. Mixture proportions (kg/m³).

Mixtures	Cement	Sand	Water	Rubber
R0	750	1050	300	0
R5	750	997.5	300	21.1
R10	750	945	300	42.2
R15	750	892.5	300	63.4
R20	750	840	300	84.5
SMR5	750	997.5	300	21.1
SMR10	750	945	300	42.2
SMR15	750	892.5	300	63.4
SMR20	750	840	300	84.5

2.4. Test methods

2.4.1. Contact angle

The hydrophobicity of the rubber particles was measured in terms of the water contact angle using a Kino s1200c contact angle measuring instrument (Kono Industry Co., Ltd.). The contact angle was used to quantify the hydrophobicity of the rubber controlling droplets within 3 μL. The terminal value of the mortar contact angle was determined using the average of three repeated measurements.

2.4.2. Flowability

The flowability of the fresh mixture was tested using a flow table according to standard ASTM C1437

of the American Society for Testing and Materials (24). The average result of three identical tests conducted on each mixture was reported.

2.4.3. Compressive strength and flexural strength

The fresh mixtures were cast using 50 mm cubic molds for the compressive strength tests according to standard ASTM C109 (25), and 40 mm × 40 mm × 160 mm prism molds were used for the flexural strength tests according to standard ASTM C349 (26). First, the mixtures were cured in the molds in the standard curing room with 23 °C ± 2 °C and RH ≥ 95%. After 24 hours, the mortars were removed from the molds and were continuously cured for 3 d, 7 d and 28 d. The average results of the triplicate specimens were reported for both the compressive strength and flexural strength tests.

2.4.4. Capillary water absorption

The capillary water absorption was measured using cylinder molds (size of d × h = 100 mm × 50 mm) according to standard ASTM C1585 (27). The specimens were cured in the curing room for 27 d. After this, except for the smooth plate surface, the other surfaces of each specimen were sealed using epoxy resin to ensure one-dimensional water transport. The specimens were oven dried to a constant weight at 105°C for 24 h. During the testing, the upper surface of the specimen was sealed with plastic film while the bottom surface was immersed in 1 - 3 mm of water. At the predetermined immersion ages, the mass of the specimen was measured and recorded. Figure 3 shows a schematic of the apparatus used for the capillary water absorption. The average value for triplicate specimens composed of each mixture was reported.

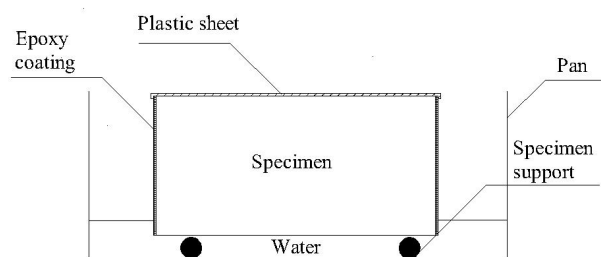


FIGURE 3. Schematic of the capillary water absorption.

2.4.5. Morphology and spectroscopy analyses

The microstructure morphology of the mortars and rubber particles (raw and surface modified) were investigated using a Flex 1000 scanning elec-

tron microscope with an acceleration voltage of 20 kV (Hitachi Co., Ltd., Japan). The prepared mortar samples cured for 28 d and the rubber particles (raw and surface modified) were sprayed with gold particles for 120 s to ensure its electrical conductivity for the SEM observations.

The mineral composition of each mixture was determined using a Smart lab SE-type X-ray diffractometer with Cu_K α radiation at 200 mA and 40 kV. The range of the scanning angle and the scan speed were $2\theta = 5^\circ - 80^\circ$ and $3^\circ/\text{min}$, respectively. The XRD specimens with particle sizes less than 75 μm were prepared from mortars cured for 28 d. Further hydration of the samples was terminated in advance by soaking the samples in anhydrous ethanol.

A Thermo Scientific Nicolet IS50 type Fourier transform infrared spectroscope was used to analyze the molecular structure of the rubber particles (raw and surface modified). Its scanning range was $4000\text{ cm}^{-1} - 400\text{ cm}^{-1}$.

3. RESULTS AND DISCUSSIONS

3.1. Morphology and contact angle of the rubber particles

The SEM images shown in Figure 4 illustrate the morphological differences between the rubber particles with and without surface modification. In Figure 4a, the raw rubber particle has a dense surface with clear corners. After the rubber particles have been surface modified using the classic Stöber sol-gel method (Figure 4b), the surfaces of the rubber particles are much rougher and are obviously different from that shown in Figure 4a, Figure 4b also shows a close-up of the surface of a rubber particle. As can be seen from the figure, the coating layer is composed of substantial spherical silica nanoparticles. This is mainly because tetraethyl orthosilicate, i.e., the silica source, was hydrolyzed and condensed to form the silica precursor solution under base catalysis. Importantly, the rubber particles act as nucleation sites and a stable silica coating is formed on the surface of the rubber particles due to a cross linking network of silica clusters and micelle's polymerization (28).

Figure 4c and Figure 4d show the contact angles between rubber particles with and without surface modification, respectively. Through surface modification by silica coating, the contact angle between the rubber particles was reduced from 120° to 103° (i.e., by 17°), which converted the surface properties of the rubber particles from strong hydrophobicity to weak hydrophobicity. This promoted hydrophilia is beneficial to achieving a better bonding efficiency between the rubber particles and the surrounding pastes.

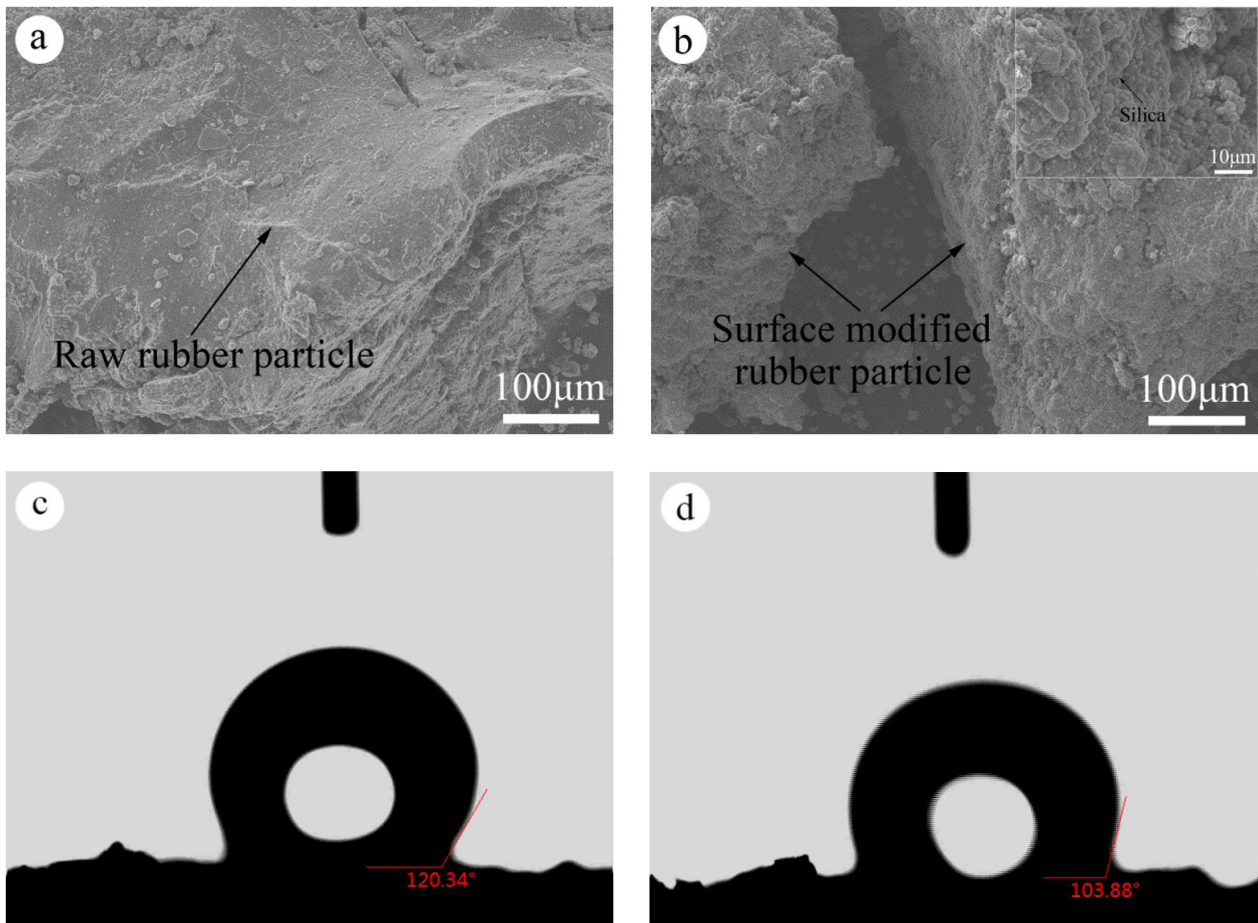


FIGURE 4. Morphology and contact angle of rubber particles: (a) SEM image of raw rubber particle, (b) SEM image of surface modified rubber particle, (c) contact angle between raw rubber particles and (d) contact angle between surface modified rubber particles.

3.2. FT-IR spectra of the rubber particles

Figure 5 shows the FT-IR spectra of the rubber particles. The major difference between the two FT-IR spectra is the existence of three peaks in the surface modified rubber's spectrum at 467 cm^{-1} , 799 cm^{-1} and 1087 cm^{-1} . In particular, the sharp peak near 467 cm^{-1} corresponds to the bending vibration peak of Si - O - Si, and the peak around 799 cm^{-1} represents the symmetric stretching vibration of Si - O. The peak at about 1087 cm^{-1} is attributed to the asymmetric stretching vibration of Si - O. These three peaks demonstrate that SiO_2 exists on the rubber sample, indicating that a layer of SiO_2 coating has been successfully applied to the surface of the rubber (29).

3.3. Flowability of the fresh mixtures

Figure 6 shows the flowability of the fresh mixtures. As can be seen from the figure, the incorporation of rubber particles into the mixtures led to poorer workabilities. The greater the amount of rubber

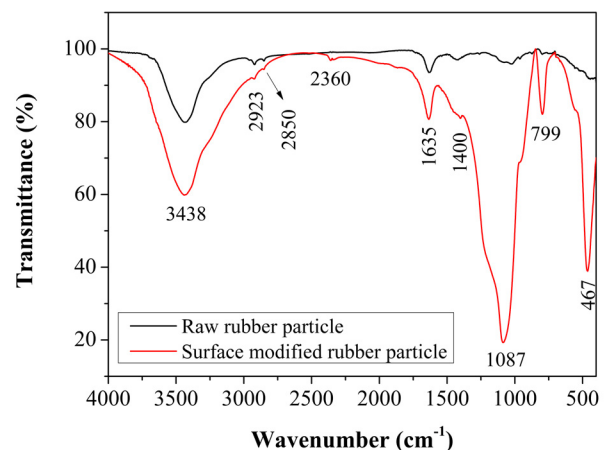


FIGURE 5. FT-IR spectra of the rubber particles.

particles, the lower the flowability. This is in agreement with the findings of Alakhras and Smadi (30). They suggested that this phenomenon was the result of gas being introduced into the fresh slurry along

with the rubber particles, which directly improved the porosity and flow resistance of the fresh slurry, resulting in the poor workability of the mortar. Nevertheless, the mortars containing surface-modified rubber particles exhibit better workabilities than the mortars containing raw rubber particles.

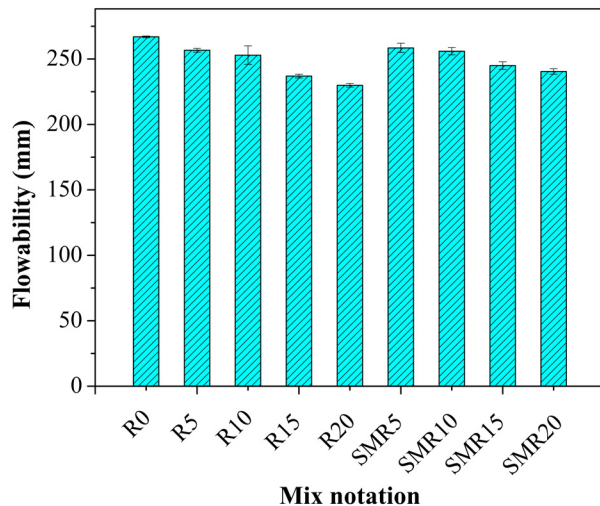


FIGURE 6. Flowabilities of the fresh mixtures.

3.4. Mechanical strength of mortars containing rubber particles

Table 3 shows the mechanical strength of the mortars containing rubber particles. Generally, the compressive strength of mortar containing rubber particles is much lower than the control group for all ages. This is reasonable and has been reported everywhere. This phenomenon occurs because the rubber particles within the microstructure of the mortar may actually act as pores due to its low

elastic modulus and the poor interface between the rubber particles and the surrounding pastes (31–33). Since the bulk property of the rubber particles is out of our control, we modified the surfaces of the rubber particles to enhance the interface and improve the mechanical strength of the mortar. As can be seen from Table 3, the compressive strengths of the mortars containing surface-modified rubber particles are significantly higher than those containing the same amount of raw rubber particles. Specially, the 28 d compressive strengths of the SMR5, SMR10, SMR15 and SMR20 mixtures were increased by 41.60%, 42.29%, 44.86% and 42.44%, respectively, compared to the corresponding mortars containing raw rubber particles. This suggests that surface coating the rubber particles helps compensate for the loss of compressive strength due to the poor surface properties of the raw rubber particles.

Table 3 also presents the flexural strengths of the mortars. The flexural strengths of the mortars containing rubber particles with or without surface modification are closely related to their compressive strengths. The addition of rubber particles with or without surface modification reduced the flexural strengths of the mortars to varying degrees. However, through surface modification, the 28 d flexural strengths of the SMR5, SMR10, SMR15 and SMR20 mixtures were increased by 7.80%, 11.17%, 20.10% and 26.28%, respectively, compared to the corresponding mortars containing the same amounts of raw rubber particles. This increment of the mechanical strength suggests that surface modification is a valid method of improving the mechanical properties of mortars containing rubber particles. This improved mechanical strength is attributed to the strengthened interface transition zone (ITZ) due to the nano silica coating. The improved hydrophilia of the modified rubber particles increases the precipitation of hydration

TABLE 3. Experimental results of the mechanical properties of mortars containing rubber particles at 3, 7 and 28 days.

Mortar specimen	Compressive strength (MPa)			Flexural strength (MPa)		
	3 days	7 days	28 days	3 days	7 days	28 days
R0	31.43(±0.79)	37.70(±0.94)	49.20(±1.26)	7.25(±0.49)	8.86(±0.30)	9.44(±0.19)
R5	22.19(±3.84)	27.24(±2.22)	34.05(±3.99)	6.29(±0.20)	7.17(±0.05)	8.55(±0.14)
R10	23.04(±1.72)	24.10(±2.47)	30.92(±1.28)	5.26(±0.13)	6.06(±0.12)	7.34(±0.13)
R15	19.82(±0.81)	20.32(±2.87)	29.67(±1.7)	5.09(±0.19)	5.85(±0.19)	6.68(±0.37)
R20	18.22(±1.58)	21.63(±1.45)	26.65(±2.02)	4.70(±0.22)	5.50(±0.25)	6.00(±0.18)
SMR5	27.80(±2.10)	32.64(±0.30)	48.22(±1.36)	6.09(±0.34)	7.48(±0.37)	9.22(±0.27)
SMR10	26.07(±6.03)	33.25(±2.46)	44.00(±2.18)	6.66(±0.17)	7.65(±0.27)	8.16(±0.34)
SMR15	24.44(±1.05)	32.00(±3.06)	42.98(±4.32)	5.71(±0.55)	6.59(±0.47)	8.02(±0.26)
SMR20	23.44(±0.17)	29.34(±1.55)	37.96(±2.04)	5.44(±0.07)	6.84(±0.11)	7.57(±0.43)

products in the region surrounding the rubber particles, and the microstructure of the ITZ becomes denser due to these additional hydration products.

3.5. Capillary water absorption

Figure 7 shows the capillary water absorption of the mortars with and without rubber particles. The capillary water absorption occurs in two stages: an initial quick stage in which the capillary water absorption is mainly controlled by open voids, and a second slow stage. In the second stage, when these open pores have been saturated, water can only be driven into the mortars through the capillary pores. The capillary tension within the capillary pores ensures that more water permeates into the mortars but at low speeds, which is classified as the slow second stage. The incorporation of raw rubber particles helps reduce the capillary water absorption of the mortar, which is ascribed to the hydrophobic nature of the rubber particles. Thus, although the incorporation of rubber particles increases the porosity of the mortars due to the poor surface conditions of the rubber particles, the capillary water absorption is substantially improved since the rubber particles impede the water permeation into the mortar (34). In contrast, the mortars containing surface-modified rubber particles have larger capillary water absorptions. For instance, the 8 d water absorption of SMR5, SMR10, SMR15 and SMR20 were larger than the corresponding mortars containing the same amounts of raw rubber particles. This difference is attributed to the improved hydrophilia of the surface-modified rubber particles in the microstructure of the mortar.

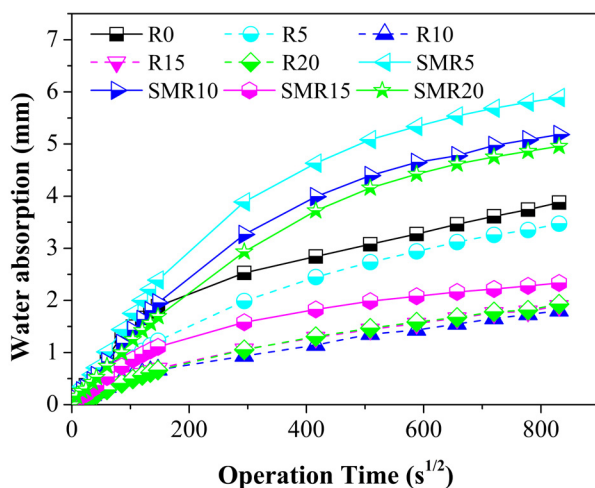


FIGURE 7. Water absorption of the mortars containing rubber particles.

3.6. Morphology and mineralogical composition

3.6.1. SEM

Figure 8 shows the SEM images of the 28 d mortars with and without rubber particles. As can be seen from Figure 8a, the microstructure of the control mortar is dense and does not contain large pores. However, as can be seen from Figure 8b to Figure 8e, the incorporation of rubber particles introduces significant pores into the microstructure of the mortars. The interfaces between the rubber particles and the surrounding pastes in these figures are obviously characterized by voids, which are shown in more detail in the close-ups. This is expected since the surface nature of the rubber particles is much more hydrophobic.

However, when the rubber particles have been surface modified by coating them with a layer of nanosilica, as can be seen from Figure 8f to Figure 8i, the microstructures of the mortars containing modified rubber particles are improved, with much fewer large pores. The voids between the surface-modified rubber particles and the surrounding pastes are smaller and more evenly disappeared. This demonstrates that the surface modification of rubber particles improves the performance of rubber mortar. As a result, strengthening the interface on microscale eventually increases the mechanical strength on the macroscale (Table 3).

3.6.2. XRD patterns

XRD analysis was conducted to investigate the influence of rubber particles on the hydration formation of cements (Figure 9). A total of five major minerals were identified and they are labeled in Figure 9, including calcium hydroxide (JCPDS # 441481), calcium silicate hydrate (JCPDS # 33-0306), gismondine (JCPDS # 200452), silica (JCPDS # 461045) and calcium carbonate (JCPDS # 170763). Among them, the diffraction peak of silica is likely caused by the sand in the mortar and the silica in the modified rubber. The calcium carbonate was likely formed through the carbonation of the calcium hydroxide during the sample preparation.

In general, the addition of rubber particles did not induce the formation of new minerals. This may be because the rubber was not involved in the hydration reaction within the mortar, and it only acted as a fine aggregate filler in the mortar. Likewise, no new substances were found in the surface modified rubber mortars. This is mainly because the silica coated on the rubber particles may be involved in the hydration reaction of the cement, and thus, it may have produced more hydrated calcium silicate rather than producing new substances. The

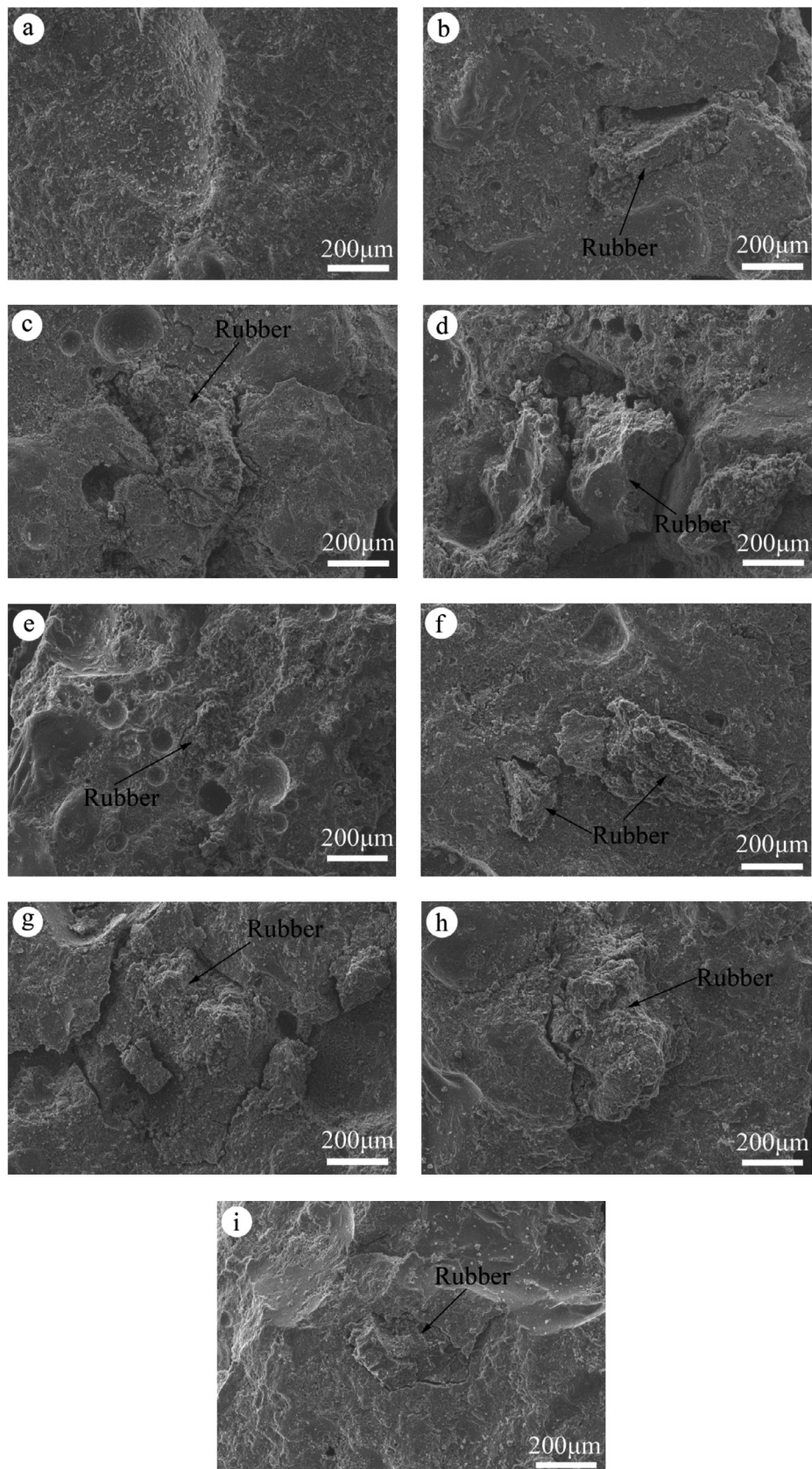


FIGURE 8. SEM images of the mortars cured for 28 days: (a) R0; (b) R5; (c) R10; (d) R15; (e) R20; (f) SMR5; (g) SMR10; (h) SMR15 and (i) SMR20.

silica coating may have a filling effect and a micro-aggregate effect, which improved the ITZ and increased the density of the structure.

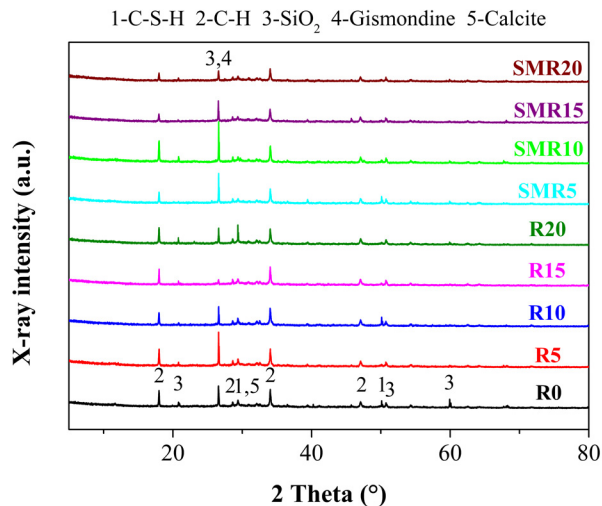


FIGURE 9. XRD spectra of the cement mortars cured for 28 days.

4. CONCLUSIONS

In this study, the effects of the surface modification of rubber particles on the performance of rubber mortars were investigated. A classical Stöber sol-gel method was used to coat the rubber particles with silica. The following conclusions were drawn from the experimental results.

1) A layer of silica coating was produced using the wet chemical sol-gel method. This coating reduced the contact angle between the rubber particles from 120° to 103° (i.e., by 17°) and modified the hydrophobic properties of the rubber from strong hydrophobicity to weak hydrophobicity.

2) The modification of the rubber particles significantly improved the mechanical strengths of the mortars from 41.60% to 44.86% (compressive strength) and from 7.80% to 26.28% (flexural strength) compared to those of mortars containing raw rubber particles depending on the dosages of the incorporated rubber particles. This confirms that the surface modification of rubber particles through chemical coating improves the mechanical properties of rubber mortars.

3) The flowabilities and capillary water absorption rates of the mortars were increased by the surface modified rubber particles as a result of the improved hydrophilia of the rubber particles within the microstructures of the mortars. However, the incorporation of surface modified rubber particles did not significantly affect the hydration products.

4) Mortars containing surface modified rubber particles have fewer pores and a much denser mi-

crostructure than mortars containing raw rubber particles. The interface between the surface modified rubber particles and the surrounding pastes was also modified.

Based on the findings of the research, the proposed modification method for rubber particles displayed promising potential towards to application in real projects in consideration of the improved workability and mechanical strength as compared to that of mortar with raw rubber particles. However, more studies should be further carried out to simplify the treatment route to achieve optimal economic efficiency.

ACKNOWLEDGMENTS

This study was funded by National Natural Science Foundation of China (52008003), Anhui Province Science and Technology Plan Project of Housing Urban-rural Construction (2020-YF12, 2020-YF14), Key Research and Development Program Project of Anhui Province (201904a07020081), and Nature Science Foundation of Anhui (1908085QE213).

REFERENCES

- Strukar, K.; Šipoš, T.K.; Miličević, I.; Bušić, R. (2019) Potential use of rubber as aggregate in structural reinforced concrete element - A review. *Eng. Struct.* 188, 452-468. <https://doi.org/10.1016/j.engstruct.2019.03.031>.
- Li, Y.; Zhang, S.; Wang, R.; Dang, F. (2019) Potential use of waste tire rubber as aggregate in cement concrete - A comprehensive review. *Constr. Build. Mater.* 225, 1183-1201. <https://doi.org/10.1016/j.conbuildmat.2019.07.198>.
- Siddika, A.; Al Mamun, M.A.; Alyousef, R.; Amran, Y.H.M.; Aslani, F.; Alabduljabbar, H. (2019) Properties and utilizations of waste tire rubber in concrete: A review. *Constr. Build. Mater.* 224, 711-731. <https://doi.org/10.1016/j.conbuildmat.2019.07.108>.
- Li, D.; Zhuge, Y.; Gravina, R.; Mills, J.E. (2018) Compressive stress strain behavior of crumb rubber concrete (CRC) and application in reinforced CRC slab. *Constr. Build. Mater.* 166, 745-759. <https://doi.org/10.1016/j.conbuildmat.2018.01.142>.
- Long, X-H.; Ma, Y-T.; Yue, R.; Fan, J. (2018) Experimental study on impact behaviors of rubber shock absorbers. *Constr. Build. Mater.* 173, 718-729. <https://doi.org/10.1016/j.conbuildmat.2018.04.077>.
- Gupta, T.; Chaudhary, S.; Sharma, R.K. (2014) Assessment of mechanical and durability properties of concrete containing waste rubber tire as fine aggregate. *Constr. Build. Mater.* 73, 562-574. <https://doi.org/10.1016/j.conbuildmat.2014.09.102>.
- Gerges, N.N.; Issa, C.A.; Fawaz, S.A. (2018) Rubber concrete: Mechanical and dynamical properties. *Case Stud. Constr. Mater.* 9, e00184. <https://doi.org/10.1016/j.cscm.2018.e00184>.
- Pham, N-P.; Toumi, A.; Turatsinze, A. (2019) Effect of an enhanced rubber-cement matrix interface on freeze-thaw resistance of the cement-based composite. *Constr. Build. Mater.* 207, 528-534. <https://doi.org/10.1016/j.conbuildmat.2019.02.147>.
- Marie, I. (2016) Zones of weakness of rubberized concrete behavior using the UPV. *J. Clean. Prod.* 116, 217-222. <https://doi.org/10.1016/j.jclepro.2015.12.096>.
- Angelin, A.F.; Cecche Lintz, R.C.; Gachet-Barbosa, L.A.; Osório, W.R. (2017) The effects of porosity on mechanical behavior and water absorption of an environmentally

- friendly cement mortar with recycled rubber. *Constr. Build. Mater.* 151, 534-545. <https://doi.org/10.1016/j.conbuildmat.2017.06.061>.
11. Li, Y.; Zhang, X.; Wang, R.; Lei, Y. (2019) Performance enhancement of rubberised concrete via surface modification of rubber: A review. *Constr. Build. Mater.* 227, 116691. <https://doi.org/10.1016/j.conbuildmat.2019.116691>.
 12. Li, G.; Wang, Z.; Leung, C.K.Y.; Tang, S.; Pan, J.; Huang, W.; Chen, E. (2016) Properties of rubberized concrete modified by using silane coupling agent and carboxylated SBR. *J. Clean. Prod.* 112 [1], 797-807. <https://doi.org/10.1016/j.jclepro.2015.06.099>.
 13. Dong, Q.; Huang, B.; Shu, X. (2013) Rubber modified concrete improved by chemically active coating and silane coupling agent. *Constr. Build. Mater.* 48, 116-123. <https://doi.org/10.1016/j.conbuildmat.2013.06.072>.
 14. Balaha, M.M.; Badawy, A.A.M.; Hashish, M. (2007) Effect of using ground waste tire rubber as fine aggregate on the behaviour of concrete mixes. *Indian J. Eng. Mater. Sci.* 14, 427-435.
 15. He, L.; Ma, Y.; Liu, Q.; Mu, Y. (2016) Surface modification of crumb rubber and its influence on the mechanical properties of rubber-cement concrete. *Constr. Build. Mater.* 120, 403-407. <https://doi.org/10.1016/j.conbuildmat.2016.05.025>.
 16. Belessiotis, G.V.; Papadokostaki, K.G.; Favvas, E.P.; Efthimiadou, E.K.; Karellas, S. (2018) Preparation and investigation of distinct and shape stable paraffin/SiO₂ composite PCM nanospheres. *Energ. Convers. Manage.* 168, 382-394. <https://doi.org/10.1016/j.enconman.2018.04.059>.
 17. Xiong, L.; Liu, J.; Li, Y.; Li, S.; Yu, M. (2019) Enhancing corrosion protection properties of sol-gel coating by pH-responsive amino-silane functionalized graphene oxide-mesoporous silica nanosheets. *Prog. Org. Coat.* 135, 228-239. <https://doi.org/10.1016/j.porgcoat.2019.06.007>.
 18. Kutysin, A.M.; Rostokina, E.Y.; Gavrishchuk, E.M.; Drobo-tenko, V.V.; Plekhovich, A.D.; Yunin, P.A. (2015) Kinetics and formation mechanism of yttrium aluminum garnet from an amorphous phase prepared by the sol-gel method. *Ceram. Int.* 41 [9], Part A, 10616-10623. <https://doi.org/10.1016/j.ceramint.2015.04.161>.
 19. Kazlauske, J.; Gårdebjer, S.; Almer, S.; Larsson, A. (2017) The importance of the molecular weight of ethyl cellulose on the properties of aqueous-based controlled release coatings. *Int. J. Pharmaceut.* 519 [1-2], 157-164. <https://doi.org/10.1016/j.ijpharm.2016.12.021>.
 20. Peng, T.; Shi, Y.; Zhu, C.; Feng, D.; Ma, X.; Yang, P.; Bai, X.; Pan, X.; Wu, C-y.; Tan, W.; Wu, C. (2020) Data on the drug release profiles and powder characteristics of the ethyl cellulose based microparticles prepared by the ultra-fine particle processing system. *Data Brief.* 29, 105269. <https://doi.org/10.1016/j.dib.2020.105269>.
 21. Jin, J.; Xiao, T.; Zheng, J.; Liu, R.; Qian, G.; Xie, J.; Wei, H.; Zhang, J.; Liu, H. (2018) Preparation and thermal properties of encapsulated ceramsite-supported phase change materials used in asphalt pavements. *Constr. Build. Mater.* 190, 235-245. <https://doi.org/10.1016/j.conbuildmat.2018.09.119>.
 22. Taguchi, Y.; Yokoyama, H.; Kado, H.; Tanaka, M. (2007) Preparation of PCM microcapsules by using oil absorbable polymer particles. *Colloid. Surface. A: Phy. Engi. Asp.* 301 [1-3], 41-47. <https://doi.org/10.1016/j.colsurfa.2006.12.019>.
 23. ASTM C150/C150M. (2018). Standard specification for Portland cement. ASTM International, West Conshohocken, PA. https://doi.org/10.1520/C0150_C0150M-18.
 24. ASTM C1437. (2013) Standard test method for flow of hydraulic cement mortar. ASTM International, West Conshohocken, PA. <https://doi.org/10.1520/C1437-13>.
 25. ASTM C109. (2013) Standard test method for compressive strength of hydraulic cement mortars (using 2-in. or [50 mm] cube specimens), ASTM International, West Conshohocken, PA. https://doi.org/10.1520/C0109_C0109M-13.
 26. ASTM C349. (2014) Standard test method for compressive strength of hydraulic - cement (using portions of prisms broken in flexure), ASTM International, West Conshohocken, PA. <https://doi.org/10.1520/C0349-18>.
 27. ASTM C1585. (2013) Standard test method for measurement of rate of absorption of water by hydraulic-cement concretes, ASTM International, West Conshohocken, PA. <https://doi.org/10.1520/C1585-13>.
 28. Yuan, H.; Bai, H.; Lu, X.; Zhang, X.; Zhang, J.; Zhang, Z.; Yang, L. (2019) Size controlled lauric acid/silicon dioxide nanocapsules for thermal energy storage. *Sol. Energ. Mat. Sol. Cell.* 191, 243-257. <https://doi.org/10.1016/j.solmat.2018.11.019>.
 29. Li, G.; Yue, J.; Guo, C.; Ji, Y. (2018) Influences of modified nanoparticles on hydrophobicity of concrete with organic film coating. *Constr. Build. Mater.* 169, 1-7. <https://doi.org/10.1016/j.conbuildmat.2018.02.191>.
 30. Al-Akhras, N.M.; Smadi, M.M. (2004) Properties of tire rubber ash mortar. *Cem. Concr. Compos.* 26 [7], 821-826. <https://doi.org/10.1016/j.cemconcomp.2004.01.004>.
 31. Angelin, A.F.; Andrade, M.F.F.; Bonatti, R.; Cecche Lintz, R.C.; Gachet-Barbosa, L.A.; Osório, W.R. (2015) Effects of spheroid and fiber-like waste-tire rubbers on interrelation of strength-to-porosity in rubberized cement and mortars. *Constr. Build. Mater.* 95, 525-536. <https://doi.org/10.1016/j.conbuildmat.2015.07.166>.
 32. Chen, X.; Wu, S.; Zhou, J. (2013) Influence of porosity on compressive and tensile strength of cement mortar. *Constr. Build. Mater.* 40, 869-874. <https://doi.org/10.1016/j.conbuildmat.2012.11.072>.
 33. Xavier, B.C.; Verzegnassi, E.; Bortolozzo, A.D.; Alves, S.M.; Lintz, R.C.C.; Gachet, L.A.; Osório, W.R. (2020) Fresh and hardened states of distinctive self-compacting concrete with marble- and phyllite-powder aggregate contents. *J. Mater. Civil. Eng.* 32 [5], 04020065.1-04020065.11. [https://doi.org/10.1061/\(ASCE\)MT.1943-5533.0003103](https://doi.org/10.1061/(ASCE)MT.1943-5533.0003103).
 34. Pham, N-P.; Toumi, A.; Turatsinze, A. (2018) Rubber aggregate-cement matrix bond enhancement: Microstructural analysis, effect on transfer properties and on mechanical behaviours of the composite. *Cem. Concr. Compos.* 94, 1-12. <https://doi.org/10.1016/j.cemconcomp.2018.08.005>.